Influence of Process Parameters and Particle Size Distribution on Mechanical Properties of Tablets

Amine Ait Ouazzou[1,*], Yogesh M. Harshe[2], Vincent Meunier[2], Jan H. Finke[3], and Stefan Heinrich[1]

DOI: 10.1002/cite.202200157

Dedicated to Prof. Dr.-Ing. Joachim Werther on the occasion of his 80th birthday

The influence of the particle size distribution of maltodextrin powders with a dextrose equivalent level of 29 as well as two tableting process variables, namely the compression pressure and the dwell time, on the tensile strength, porosity, and pore size distribution of the final tablet was studied. The mechanical strength and porosity of the tablets are assessed in relation to the powder and process parameters. Regarding the process parameter, it was show that the compaction pressure clearly has a more pronounced influence on the tablet porosity and mechanical strength compared to the influence of the dwell time in the range of the study. As a result, the study offers a better understanding of how the properties of a tablet are influenced by the inter-correlation of powder characteristics and tableting parameters. Therefore, the shelf-life studies and tablet downstream processing as well as drug product development will benefit greatly from this work.

Keywords: Diametral crushing, Maltodextrin, Porosity, Tableting, X-ray tomography

Received: August 01, 2022; *revised:* November 23, 2022; *accepted:* December 05, 2022

1 Introduction

Powders are widely utilized in a variety of industries, including the food, pharmaceutical, and chemical sectors [1]. Therefore, it is essential to guarantee that powder behaviours are described to ensure consistent product quality whether utilized as dry powder or while reconstituting. Powders frequently undergo the unit process of tableting to aid in storage, transportation, handling, and dosing [2]. The intended usage of the tableted powders might vary greatly from industry to industry [3].

Tableting is a compression process, which consists of applying a uniaxial force on a powder that has been filled into a confined space [2]. Particle size distribution as well as process parameters such as dwell time and compaction force has been reported to have an influence on the mechanical strength and porosity of tablets [4, 5].

A solid material's physical behaviour is strongly influenced by its supra-molecular structure. Molecules may take either a highly ordered structure, as seen in crystalline materials, or a statistically non-equilibrium arrangement as observed in amorphous materials [6]. In this study, a focus was put on amorphous powders with the use of maltodextrin as a model system.

During the tableting process many phenomena may occur depending on the material properties. These phenomena include particle rearrangement, mechanical interlocking, particle breakage and deformation, all of which lead to the creation of bonds between particles by increasing the particle-particle contacts [4, 7].

Particle size distribution as well as process parameters such as compaction force and dwell time have shown to have an influence on the compressibility, tabletability and compatibility of powders [5, 8]. However, the influence of particle size distribution is not yet fully understood, with some studies attesting of the strong influence on the mechanical properties of the tablet [9] and other reporting limited to no influence [10]. Therefore, is it important to assess the influence of particle size distribution and process parameters for a widely used powder such as maltodextrin.

[1]Amine Ait Ouazzou, Prof. Dr.-Ing. habil. Dr. h.c. Stefan Heinrich (amine.ait.ouazzou@tuhh.de)
Institute of Solids Process Engineering and Particle Technology, Hamburg University of Technology, Denickestraße 15, 21073 Hamburg, Germany.

[2]Dr. Yogesh M. Harshe, Dr. Vincent Meunier
Nestlé Research, Route du Jorat 57, Lausanne 1000, Switzerland.

[3]Dr. rer. nat Jan H. Finke
Institute for Particle Technology and Center of Pharmaceutical Engineering – PZV, Technical University of Braunschweig, Germany.

2 Materials and Methods

2.1 Maltodextrin

Maltodextrin in the form of dried glucose syrup under the brand name Glucidex from the company Roquette Frères (Lestrem, France) was used for the study. It is a polysaccharide that consists of several D-glucose units in chains of variable lengths, and it is typically categorized based on the dextrose equivalent or DE level of the powder. The higher the DE level the shorter the glucose chains, hence the molecular weight is lower for high DE levels. Consequently, monomeric glucose has a DE of 100 whereas starch has a DE of 0. Glucidex is produced by enzymatic hydrolysis. This process produces a maltodextrin consisting of several DE levels, therefore the products ordered from Roquette will be within a range of DE levels instead of an exact value [4]. Roquette also provides dried glucose syrup of the same DE level but with different particle size distribution under the name extension "D" or "IT" for the agglomerated version. For this study the powders 29D and 29IT have been used. These powders are dried glucose syrup with the same chemical structure at DE level 29, with the IT being the agglomerated version of the D. The IT powder is agglomerated using wet granulation in fluid bed with water.

2.2 Tableting

The tableting experiments were conducted on the STYL'One Evo compaction simulator as show in (Medel'Pharm, Beynost, France). The tableting process was performed by changing the dwell time and compaction force. Sodium stearyl fumarate (PRUV®, JRS Pharma, Rosenberg, Germany) was used as a lubricant by adding 0.5 % to a 250 g batch of glucose syrup and mixing for 2 min in a Turbo 3D Mixer (Tuburbula, Willy A. Bachofen, Muttenz, Switzerland). The punches were biplanar and followed a linear compaction profile until reaching the desired compaction force (5 kN, 10 kN, 20 kN, 30 kN, 40 kN). The die used was cylindrical with a diameter of 14 mm and was filled to a height of 15 mm. The software Analis provided by Medel'Pharm was used for the analysis and monitoring, and for all other post-processing a python script was used. Fig. 1 shows a typical tableting process for two different dwell times a) 1 ms and b) 1000 ms.

The most well-known equation expressing the connection between porosity and pressure is the Heckel equation [11]. The basis for Heckel equation Eq. (1) is that the compression of powders is comparable to a first-order chemical reaction, with the pores serving as the reactant and densification of the bulk as the result. The equation was initially created and used to describe compression of metals, which are known to primarily deform plastically:

$$\ln\left(\frac{1}{1-D}\right) = KP + A \tag{1}$$

With K and A being Heckel's equation parameters, P the compaction pressure (Pa) and D the solid fraction.

After the tableting experiment, the tablets were stored in sealed aluminium bags in order to avoid any deterioration due to humidity.

2.3 Porosity Measurements

The skeletal volume of the powder has been measured using a helium pycnometer (Accupyc II 1340, Micromeritics, United States). The true density of the material ρ_{material} is then computed using the known weight of the sample and the volume of powder, which can be computed at this point. The true density ρ_{material} was obtained from a sample of grinded 29D powder, the value was 1.55 g cm^{-3} for the 29D and 29IT, since both powders are chemically identically. Each measurement point has been performed on three tablets.

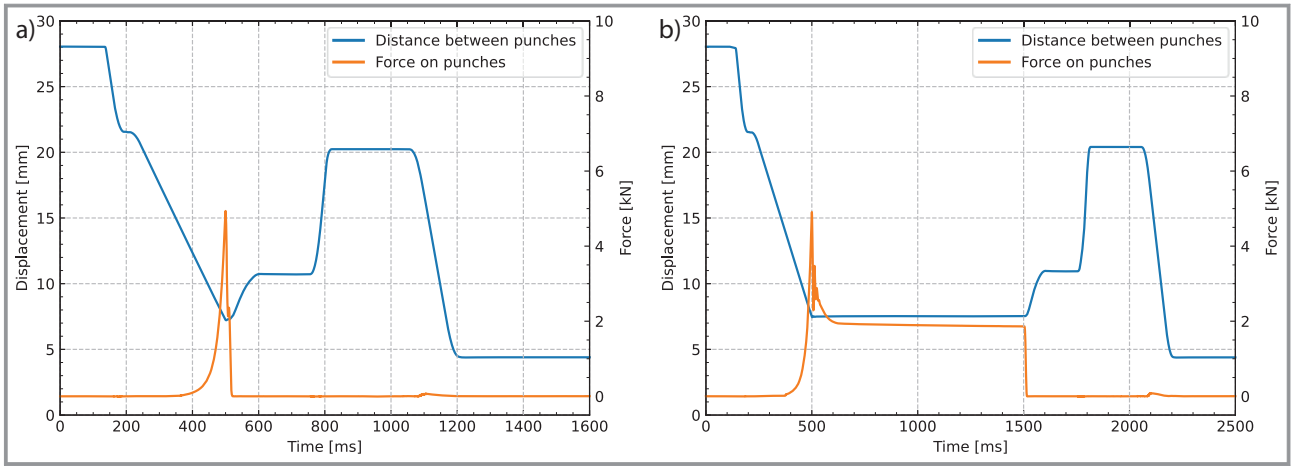

Figure 1. Tableting process 29IT. a) 5 kN at 1 ms dwell time, b) 5 kN at 1000 ms dwell time.

The porosity of the tablet ε was computed as show in Eq. (2):

$$\varepsilon = 1 - \frac{\rho_{\text{tablet}}}{\rho_{\text{material}}} \quad (2)$$

The ρ_{tablet} was obtained by measuring the mass of the tablets and their height after slow elastic recovery (1 month after tableting experiments). The radial relaxation was neglected. Both open and closed pores contributed to the density of the tablets. The analysis of the porosity/solid fraction is required for this study since it is a crucial parameter that can affect both a tablet's strength [8] and its dissolution characteristics [12].

2.4 Pore Size Distribution

2.4.1 X-ray Microtomography

X-ray tomography was used to qualitatively study the pore structure of the tablets, through this technique some of internal geometrical and topological properties of the tablet's pore structure can be assessed. For this study, a Micro-CT (Scanco µCT 35, SCANCO Medical AG, Switzerland) was used with 45 kVp, 177 µA and 8 W with a test tube of 20.5 mm diameter, this meant that the resolution obtained was a voxel of 10 µm. The image processing was performed with a python script, by converting the DICOM images to Hounsfield units as shown in Fig. 2 and applying a low-pass filter with a cut-off value of –300 HU, where any pixel above –300 HU is converted to white pixels and all values of under –300 HU to black pixels. This value was chosen in order to reproduce the global porosity that has been measured previously.

2.4.2 Mercury Intrusion

Mercury intrusion (Auto Pore III bis 414 MPA, Micromeritics, United States) is a measurement technique that helps determine pore size distribution, using a non-wetting liquid. It can determine pore sizes as small as 3 nm depending on the contact angle of mercury with a solid measured. This is achieved by putting the tablet in a container that is then vented to reach a vacuum condition, then the mercury

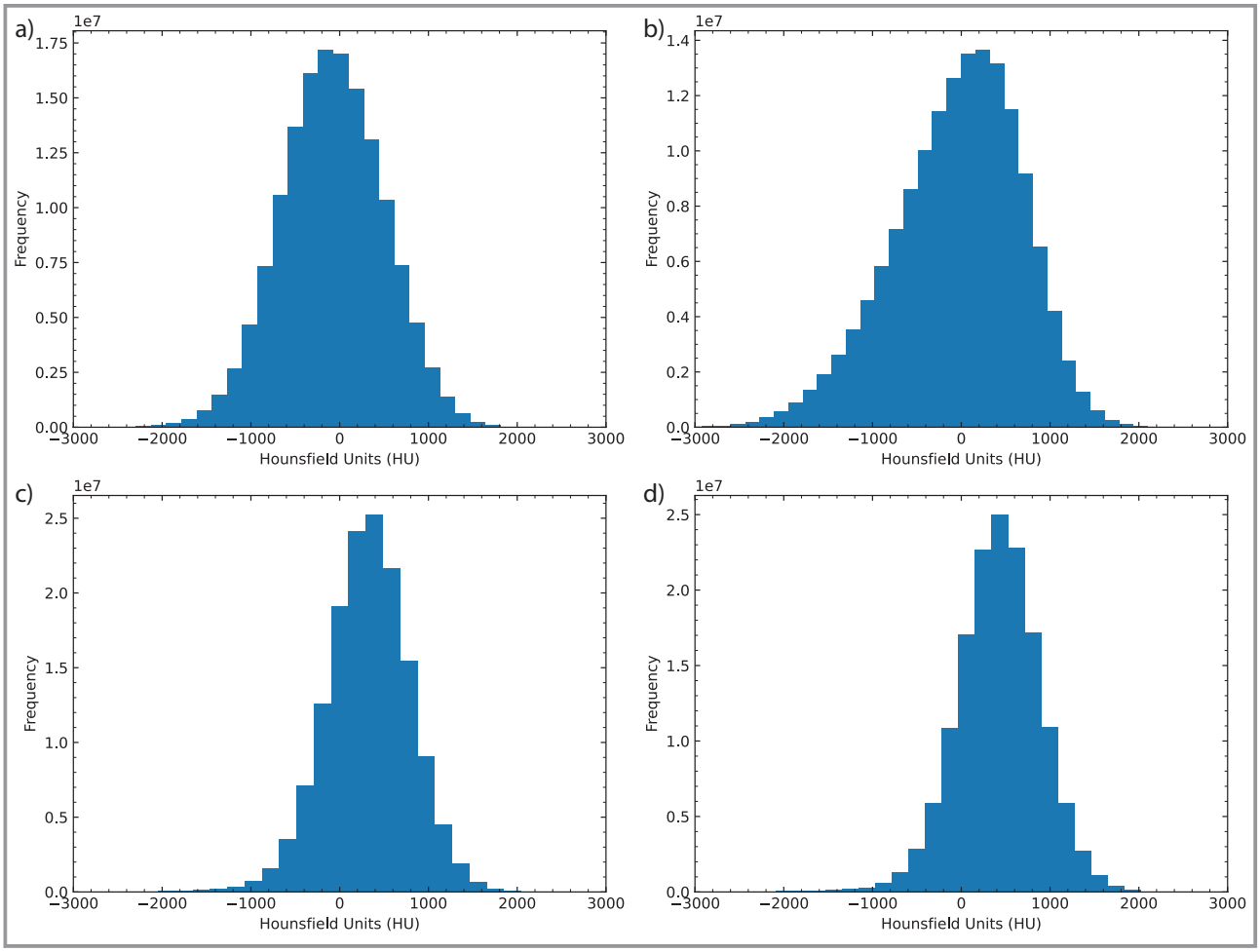

Figure 2. Distribution of the pixel's frequency converted in Hounsfield units. a,b) 29D & 29IT at dwell time 100 ms and compaction force 5 kN, respectively; c,d) 29D & 29IT at dwell time 100 ms and compaction force 40 kN, respectively.

is gradually injected, in order to allow the setup to reach an equilibrium and therefore avoid destroying the tablet. The pore sizes are then related to the pressure measured in the container by the Washburn's equation Eq. (3) [13] by assuming the contact angle θ to be 140° [14]:

$$D = \frac{-4\,\gamma\cos(\theta)}{P} \tag{3}$$

D being the diameter of pores (m), γ the surface tension of mercury was taken from literature to be (0.48 N m^{-1}) [14] and P the pressure (Pa).

2.5 Diametral Crushing Test

The test has been conducted with a texture analyser (stable micro systems, United Kingdoms). A tablet was placed between two flat surfaces and a force was exerted until the tablet broke, the upper plate was travelling at a constant speed of 0.1 mm s^{-1}. All the values up to the breakage point have been recorded, the trigger weight has been set to 0.5 g. Each measurement point has been performed on three tablets.

The tensile strength σ of the tablets was determined from the maximum compression force by assuming the clean axial breakage of each tablet with the following Eq. (4) [15]:

$$\sigma = \frac{F_{\max}}{\pi r h} \tag{4}$$

with σ the tensile strength of the tablet (Pa), $F_{\max}$ the maximum force recorded (N), r and h the radius and height of the tablet, respectively (m).

2.6 Elastic Recovery

Elastic recovery is generally described as the ability of a material to recover its original form after a load has been applied and lifted. In this study the elastic recovery of the tablets has been computed as show in Eq. (5) [5] and each measurement point has been performed on three tablets:

$$ER = \frac{h_{\max} - h_{\min}}{h_{\min}} \tag{5}$$

$h_{\min}$ being the distance between punches at maximum compression force (m), $h_{\max}$ is the height of tablets (m) measured after relaxation (1 month after tableting experiments), ER is the elastic recovery (%).

3 Results and Discussion

3.1 Powder Characterisation

3.1.1 Particle Size Distribution

The particle size distribution of both powders as shown in Fig. 4 has been determined using the CAMSIZER XT dynamic image analysis system (Retsch GmbH, Haan, North Rhine-Westphalia, Germany) with a dispersion pressure of 200 kPa for the 29D powder and 50 kPa for the 29IT powder, in order to avoid breaking the agglomerates. The 29D powder has a wider distribution with smaller particles as opposed to the 29IT powder that has a narrower distribution with bigger particles, indicated by the Span $(d_{90}–d_{10})/d_{50}$. Tab. 1 describes the d_{10}, d_{50}, d_{90} and the span of both particle size distributions for 29D and 29IT. In Fig. 3, SEM images taken on the Zeiss Supra VP55 (Carl Zeiss AG, Oberkochen, Germany) of both powders are

Table 1. Size classes of powders used.

Class size [µm]	d_{10}	d_{50}	d_{90}	Span
29D	28.0	99.0	201.7	1.75
29IT	130.6	254.5	410.2	1.10

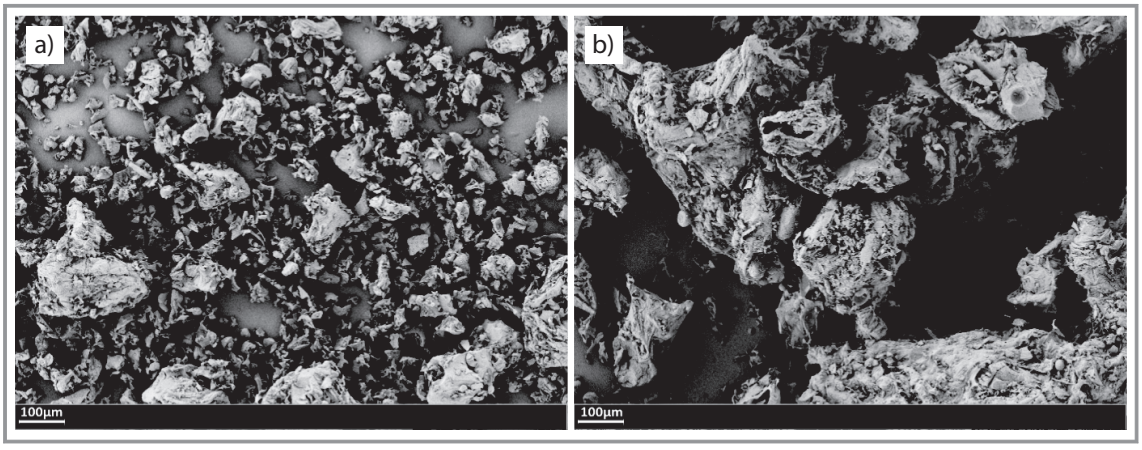

Figure 3. SEM images of maltodextrin powders a) 29D, b) 29IT.

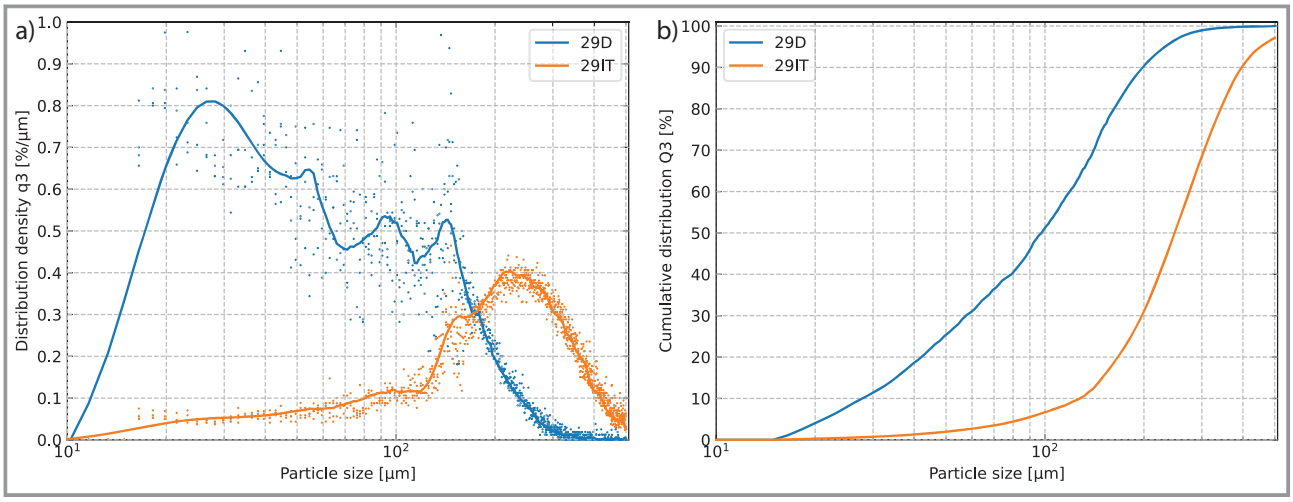

Figure 4. Particle size distribution of maltodextrin powders. a) Density function, b) cumulative function.

shown in order to highlight the size difference and the shape of the particles.

3.1.2 Moisture Content and Water Activity

The moisture content of both powders has been measured using a Moisture analyser DAB with 1 g samples heated at 105 °C for 30 min. The water activity was read from the sorption isotherm of maltodextrin DE 29 that was measured by Nestlé scientists and reported in the dissertation of Julien Dupas [16]. Tab. 2 summarizes these results.

Table 2. Powder moisture content and water activity.

	Moisture content [%]	Water activity [–]
29D	3.15 ± 0.10	0.15 ± 0.01
29IT	4.92 ± 0.10	0.21 ± 0.01

3.2 Tableting Process

Three separate sections may often be used to identify a Heckel profile [17]: a non-linear beginning (region I), followed by a linear segment (region II), and a nonlinear section (region III). These three zones are frequently explained by the underlying rate-controlling compression processes that are dominant in each of them. For region I, there are two main theories put forth: the first holds that the curvature is based on particle rearrangement during compression, while the second holds that the curvature is based on particle fragmentation. It is commonly acknowledged that particle deformation, whether elastic or plastic, controls the process of powder compression in region II. Finally, it is suggested that in region III elastic deformation of the compact regulates the process.

It is shown in Fig. 5 that the 29IT powder is resisting change less with the raise of compaction pressure than the

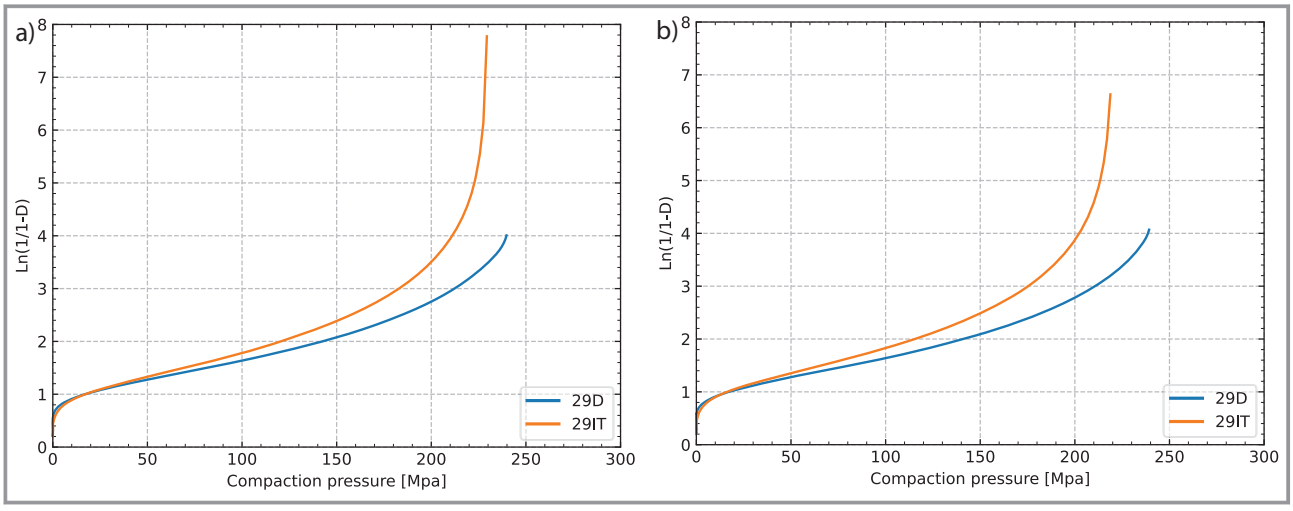

Figure 5. Heckel's plot. a) Powders compacted at 40 kN and 1 ms dwell time, b) powders compacted at 40 kN and 1000 ms dwell time.

29D powder. At a lower compaction pressure, we cannot see any relevant differences between both powders. However, as the compaction pressure gets higher, the difference in response to stress of both powders grows bigger, as we can see the gap between the two curves widening.

With respect to dwell time, by comparing Fig. 5a to 5b we notice that the differences between the compaction behaviour of both powders is increasing with the increase of dwell time, however this should not be the case since the heckle plot has only been plotted till the highest compaction force (namely 40 kN), meaning that the dwell time should not affect the results. The tablets for 1 ms and 100 ms have been produced in different batches, which introduces some disparities, that are shown in the heckle plot particularly towards the higher compaction pressures. This is due to the fact that at higher pressures the tablet is at its highest density and is approaching the material true density, meaning that the relative density approaches 1, which then translates to high values in the heckle plot, and high sensitivity in the graph, simply due to the form of Eq. (1).

This result is then found in the elastic recovery behaviour of the tablets Fig. 6. We find that the elastic recoveries of tablets produced with both powders have similar percentages at lower pressures, but as the compaction pressure grows, the tablets produced with 29D powder tend to recover more of their thickness than the ones produced with 29IT powder. This could be explained by the fact that the initial filling of the die was performed with a constant volume, which leads to a difference in the number of particles due to the fact that the powders have different particle size distribution and therefore different packing behaviours leading to two distinct bulk densities 0.51 g cm^{-3} and 0.47 g cm^{-3} for 29D and 29IT, respectively. This causes more particle-particle contact to happen in 29D than in 29IT, which is then translated to a higher resistance to the compaction process and therefore more potential energy stored under the form of elastic deformation of the particles. This energy is released in a form of expansion, hence the higher elastic recovery for the 29D tablets.

Regarding the effect of dwell time, we notice by comparing Fig. 6a and 6b that there is a decrease in the elastic recovery with the increase of dwell time, this influence is more easily observed at higher compaction forces. This can be due to the fact that part of the energy stored is being dissipated when the compaction force is held for a longer period of time, which leads to a lower elastic recovery.

3.3 Tablet Mechanical Properties

Tabletability, compactibility, and compressibility [18] profiles are often used in the pharmaceutical industry to describe raw materials and powder formulations under compression [19]. It is feasible to interpret the mechanical behaviour of the tested materials throughout the compression process by analysing these profiles (compression performance) [20]. The correlation between pressure and tablet strength is explained by the tabletability profile. When other factors impacting the process, including porosity are taken into consideration, compactibility and compressibility provide additional information to characterize the overall compression behaviour.

The ability of a powdered substance to form a tablet of a specific strength when subjected to compaction pressure is known as tabletability. As it is shown in Fig. 7a and 7b compaction pressure has a strong influence, where we notice a considerable increase in tablet strength with increasing compaction pressures. Regarding the influence of the dwell time, we notice that with higher values higher tabletability is achieved. The effect on PSD is also to be considered as the larger powder with a narrower PSD (29IT) achieves a higher level of tabletability compared to the smaller and wider PSD powder (29D).

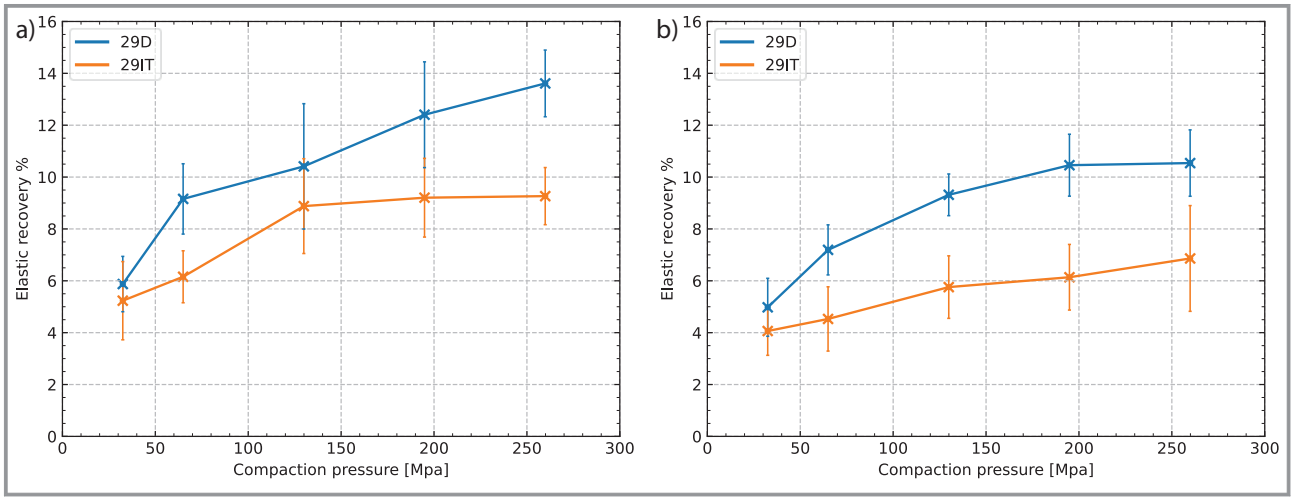

Figure 6. Elastic recovery for 29D and 29IT for several compaction pressures at 1 ms (a) and 100 ms (b) dwell time.

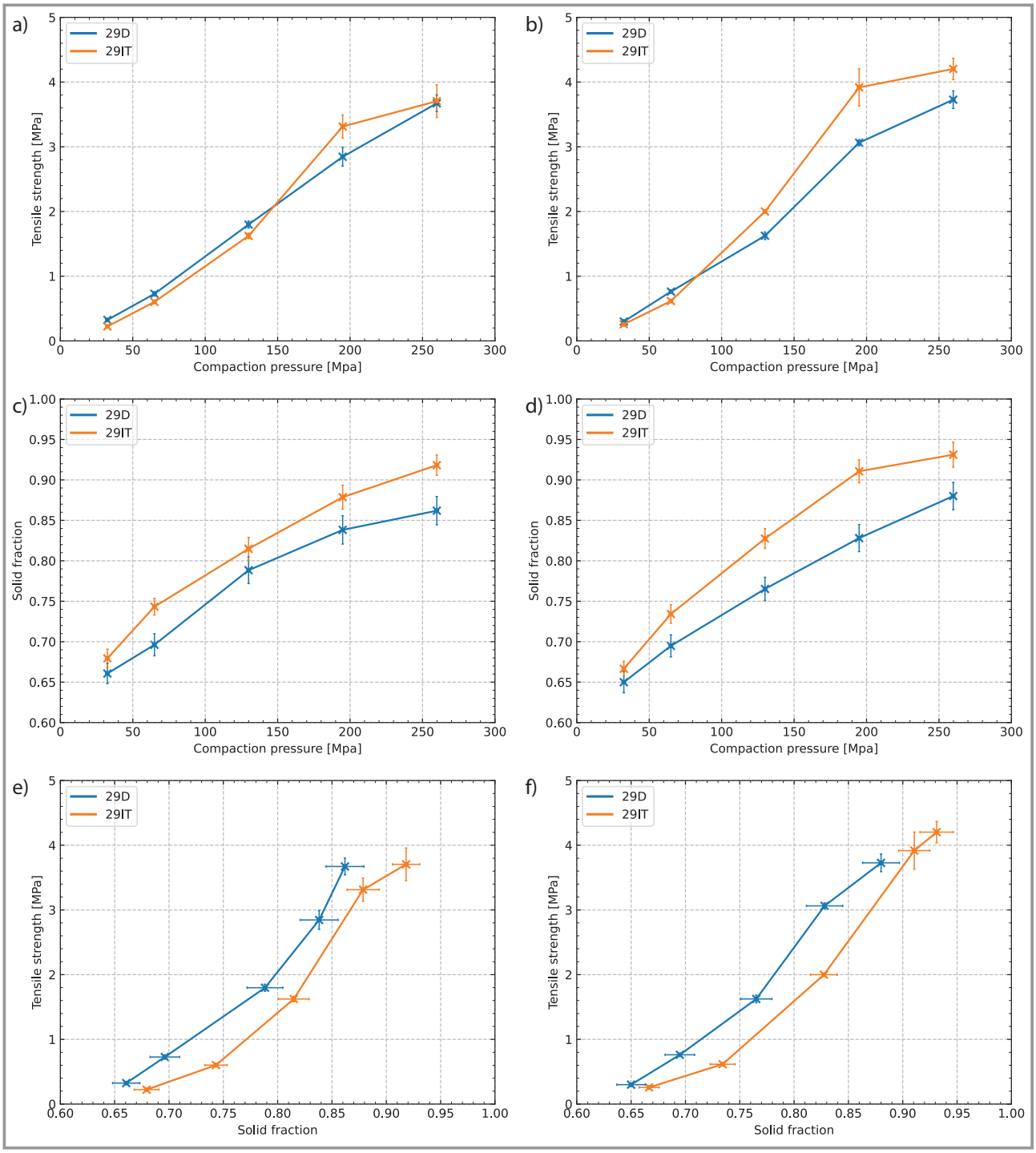

Figure 7. Tabletability (a,b), comprssibility (c,d) and compactibility (e,f) for 29D and 29IT at 1 ms and 1000 ms dwell time, respectively.

Compressibility is the capacity of a powder to shrink in volume when subjected to pressure. It describes how easily a powder changes volume when compressed. It is usually assessed by plotting the porosity or solid fraction of tablets over the applied compaction pressure.

Compactibility, on the other hand, is the ability to produce tablets having a certain strength at a specific solid fraction. It is therefore evaluated by plotting the tensile strength of tablets with respect to the solid fraction.

From Fig. 7c and 7d it can be seen that both powders reach a higher solid fraction, when compacted with a higher compaction pressure and dwell time. The effect of PSD is also to be considered since tablets produced from 29IT powder reach a higher solid fraction than 29D tablets.

In Fig. 7e and 7f we can observe the dependence of strength for a given solid fraction for two different powders. From the results obtained it can be noted that a tablet produced with 29D powder consistently achieves a higher tensile strength than the 29IT powder for the same solid fraction. This can also be explained with the fact that there are more particles interacting in a 29D tableting process than in 29IT, which then leads to a creation of a considerably higher number of solid bridges between particles for the same solid fraction reached by both tablets. However, as it is shown in the previous graphs, the 29D powder is required to be compacted at a higher pressure in order to achieve similar solid fraction as for a tablet with 29IT powder.

In [5], the authors state that the initial particle size distribution does indeed influence the mechanical properties of a tablet but also the compaction process. The authors state that a powder with a smaller particle size tends to resist the compression more than the powder with a bigger particle size. This has also been found to be the case for maltodextrin with the 29D powder (smaller particle size) resisting compression more than the 29IT powder (bigger particle size). The authors also state that a powder with a smaller particle size tends to produce stronger tablets. This result is also consistent with the results of this study, as it was demonstrated that at the same solid fraction the 29D (smaller particle size) produces stronger tablet than the 29IT powder (bigger particle size).

3.4 Tablet Porosity

Tablet porosity is a crucial characteristic that has a significant impact on how well a tablet performs with respect to different postprocessing operation. By assessing porosity, the manufacturer may produce tablets that meet important requirements ranging from shelf life, dissolution rates to mechanical properties. In addition to determining the global porosity, it is important to have information about the pore sizes and their spatial distribution within tablets. In this study we focused on quantifying the pore size distribution with both X-ray tomography and mercury intrusion, to have a qualitative and quantitative understanding of the pore size distributions and how they are influenced by process parameters and powder characteristics [21].

As it was shown in previous plots the porosity is decreased by raising the compaction pressure. However, the Micro-CT measurements show that the pore size distribution is also affected by compaction pressure. From Fig. 8a we can see that the larger pores completely disappear, and the proportion of small pores is also reduced. By plotting the normalized cumulative distribution, we can assess the contribution of several pore sizes to their respective global void fraction, therefore in Fig. 8b it is observed that despite the difference in global porosity between tablets produced at 5kN with both 29D and 29IT powder, the proportion of pore size categories to their global tablet porosity is quite similar for both powders. However, there starts to be a distinction between these distributions at higher compaction pressure, with small pores representing a bigger portion of the global porosity for the 29IT tables than for the 29D tablets.

In Fig. 9, the cumulative pore size distribution and the log differential intrusion of mercury are presented respectively. It is evident by comparing the pore size distribution from Fig. 9a and Fig. 8a that the sizes that have been measured with the Micro-CT were overestimating the sizes of the pores. This is due to the low resolution achieved as well as the post-processing of the images, where although the global porosity was retrieved, the pore sizes were overestimated. However, the trends of the curves were fairly accurate compared with the mercury intrusion trends in Fig. 9a. Hence, Micro-CT can still be used in order to run a qualitative study as a non-intrusive method to yield global porosity. From Fig. 8 it is clear that with the increase of compaction

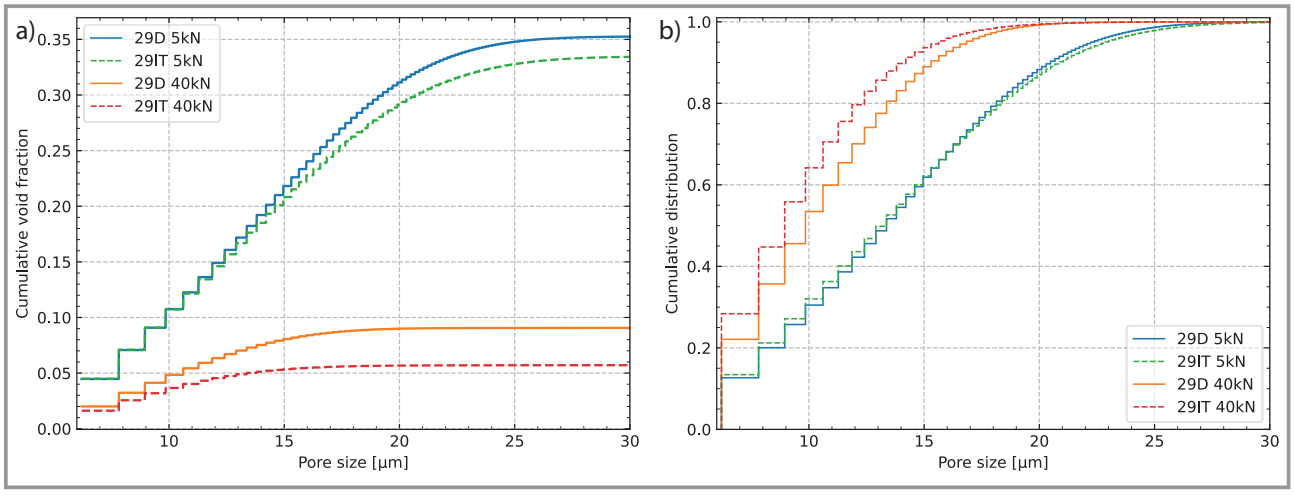

Figure 8. Pore size distributions from Micro-CT. a) Cumulative pore size distribution, b) normalized cumulative pore size distribution at dwell time 100 ms.

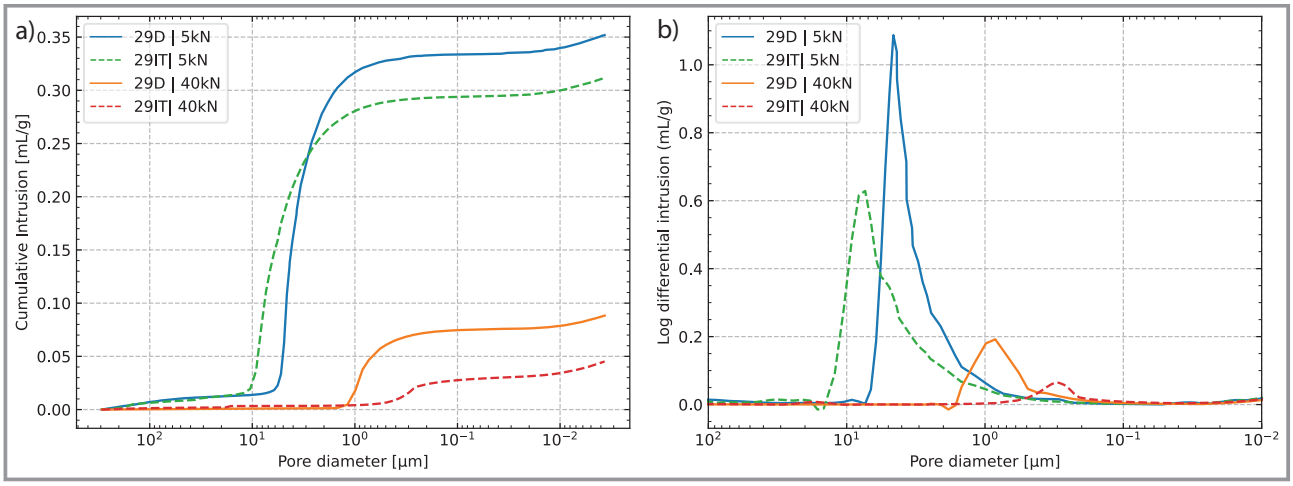

Figure 9. Cumulative pore size distribution (a), and log differential intrusion (b) at dwell time 100 ms from mercury intrusion.

pressure the pore sizes are globally reduced with some sizes completely disappearing. It is also important to point out that despite the fact that the global porosity of the 29IT tablets is lower than of the 29D tablets, the sizes of the pores for the 29IT tablet tend to be bigger than the 29D tablets at low compaction pressures, and smaller when the compaction pressure is higher. This effect is clearly visible in Fig. 9b and might be explained by the fact that the 29IT powder has a lower resistance to change than the 29D powder (Fig. 5). The global porosity was also retrieved from the mercury intrusion measurements, which suggests that the overwhelming majority of pores are "open pores", which are in one way or another connected to the surface of the tablet.

As reported by [21] the Micro-CT did underestimate the smaller pore sizes. However, unlike in [21], the global porosity has been retrieved in this study because a different post-processing of the images was conducted. Ultimately, the results of this study agree with [21] and both show that the Micro-CT can indeed be used for studying the inner structure of a tablet and determine to a certain extent the pore size distribution.

4 Conclusion

In this study we have shown how compaction pressure and dwell time can influence the overall mechanical properties of a tablet. It was demonstrated that out of all the parameters studied, compaction pressure is the most influential factor impacting the tablet mechanical properties. However, particle size distribution also influenced strongly both the mechanical properties of powders and the pore size distribution. The dwell time although being an influential parameter has considerably less impact than the other parameters.

This study has provided a better understanding of the tableting process and its driving parameters, which is crucial for both the pharmaceutical industry and the food industry in the product development phase to produce tablets from lose powders. It also provides some valuable input for future studies that involve modelling of the tableting process with means of discrete element method.

This project has received funding from the European Union's Horizon 2020 research and innovation programme under the Marie Sklodowska-Curie grant agreement No 955661. Open access funding enabled and organized by Projekt DEAL.

Symbols used

A	[–]	Intercept of Heckel's plot
D	[m]	Particle diameter in Washburn's equation
D	[–]	Solid fraction in Heckel's plot
d_x	[µm]	Particle size (diameter) when the cumulative percentages reaches x %
ER	[%]	Elastic recovery
F_{max}	[N]	Maximum breakage force recorded
h, h_{max}	[m]	Height of tablet measured (1 month after tableting experiments)
h_{min}	[m]	Distance between punches at maximum compression force
K	[MPa^{-1}]	Slop of Heckel's plot
P	[MPa]	Compaction pressure
r	[m]	Radius of tablet taken constant

Greek letters

ε	[–]	Porosity
σ	[MPa]	Tensile strength
ρ_{tablet}	[g cm^{-3}]	Density of tablet

$\rho_{material}$	[g cm^{-3}]	Density of material/ True density
γ	[N m^{-1}]	Surface tension
θ	[°]	Contact angle

Abbreviations

PSD Particle size distribution

References

[1] J. J. Fitzpatrick, L. Ahrné, *Chem. Eng. Process.* **2005**, *44 (2)*, 209–214. DOI: https://doi.org/10.1016/j.cep.2004.03.014

[2] S. Jain, *Pharm. Sci. Technol. Today* **1999**, *2 (1)*, 20–31. DOI: https://doi.org/10.1016/S1461-5347(98)00111-4

[3] J. Dupas, V. Girard, L. Forny, *Langmuir* **2017**, *33 (4)*, 988–995. DOI: https://doi.org/10.1021/acs.langmuir.6b04380

[4] W. R. Mitchell, L. Forny, T. Althaus, D. Dopfer, G. Niederreiter, S. Palzer, *Chem. Eng. Sci.* **2017**, *167*, 29–41. DOI: https://doi.org/10.1016/j.ces.2017.03.056

[5] I. Wünsch, J. H. Finke, E. John, M. Juhnke, A. Kwade, *Int. J. Pharm.* **2021**, *599*, 120424. DOI: https://doi.org/10.1016/j.ijpharm.2021.120424

[6] S. Palzer, *Trends Food Sci. Technol.* **2010**, *21 (1)*, 12–25. DOI: https://doi.org/10.1016/j.tifs.2009.08.005

[7] S. Palzer, *Agglomeration of food powders*, Habilitation thesis, TU Munich **2007**.

[8] A. Adolfsson, C. Nyström, *Int. J. Pharm.* **1996**, *132 (2–3)*, 95–106. DOI: https://doi.org/10.1016/0378-5173(95)04336-5

[9] J. S. Kaerger, S. Edge, R. Price, *Eur. J. Pharm. Sci.* **2004**, *22 (2–3)*, 173–179. DOI: https://doi.org/10.1016/j.ejps.2004.03.005

[10] K. S. Khomane, A. K. Bansal, *AAPS PharmSciTech* **2013**, *14*, 1169–1177. DOI: https://doi.org/10.1208/s12249-013-0008-4

[11] D. Hooper, F.C. Clarke, *J. Nanomed. Nanotechnol.* **2016**, *7 (3)*. DOI: https://doi.org/10.4172/2157-7439.1000381

[12] M. Riippi, J. Yliruusi, T. Niskanen, J. Kiesvaara, *Eur. J. Pharm. Biopharm.* **1998**, *46 (2)*, 169–175. DOI: https://doi.org/10.1016/S0939-6411(98)00003-4

[13] E. W. Washburn, *Proc Natl Acad Sci USA* **1921**, *7 (4)*, 115–116. DOI: https://doi.org/10.1073/pnas.7.4.115

[14] P. J. Dees, J. Polderma, *Powder Technol.* **1981**, *29 (1)*, 187–197. DOI: https://doi.org/10.1016/0032-5910(81)85016-4

[15] J. T. Fell, J. M. Newtont, *J. Pharm. Sci.* **1970**, *59 (5)*, 688–691. DOI: https://doi.org/10.1002/jps.2600590523

[16] J. Dupas, *Wetting of soluble polymers*, Ph.D. thesis, Université Pierre et Marie Curie – Paris **2012**.

[17] M. U. Ghori, *Br. J. Pharm.* **2016**, *1 (1)*. DOI: https://doi.org/10.5920/bjpharm.2016.09

[18] M. Drašković, J. Djuriš, S. Ibrić, J. Parojčić, *Powder Technol.* **2018**, *326*, 292–301. DOI: https://doi.org/10.1016/j.powtec.2017.12.021

[19] A. Adolfsson, C. Nyström, *Int. J. Pharm.* **1996**, *132 (2–3)*, 95–106. DOI: https://doi.org/10.1016/0378-5173(95)04336-5

[20] C. K. Tye, C. Sun, G. E. Amidon, *J. Pharm. Sci.* **2005**, *94 (3)*, 465–472. DOI: https://doi.org/10.1002/jps.20262

[21] A. K. Schomberg, A. Diener, I. Wünsch, J. H. Finke, A. Kwade, *Int. J. Pharm.: X* **2021**, *3*, 100090. DOI: https://doi.org/10.1016/j.ijpx.2021.100090

